RF safety assessment of a bilateral 4-channel Tx/Rx 7T breast coil

Thomas M Fiedler[1], Aaron S Kujawa[1], Frank Resmer[2], Patrick Stein[2], Titus Lanz[2], Mark E Ladd[1,3], and Andreas K Bitz[1]

[1]*Medical Physics in Radiology, German Cancer Research Center (DKFZ), Heidelberg, Germany,* [2]*RAPID Biomedical GmbH, Rimpar, Bavaria, Germany,* [3]*Erwin L. Hahn Institute for Magnetic Resonance Imaging, University Duisburg-Essen, Essen, Germany*

Target audience: Researchers involved in RF safety and/or high-field MRI

Introduction: MRI is an important tool for diagnosis of breast cancer. Local RF coils have to be used due to the lack of a body resonator in 7 T MR scanners to evaluate the clinical benefit of the increased SNR at 7 T for breast imaging. The shorter wavelength at 7 T increases the non-uniformity of the effective excitation field (B_1^+) as well as the local energy absorption in the tissue. Hence, optimization of the transmit field in addition to a reliable RF safety evaluation of the RF coil is essential. To this end, RF simulations based on an exact model of the breast coil and an anatomical heterogeneous body model can be used to obtain realistic specific absorption rates (SAR). This information allows operation of the transmit coil at optimum performance. In this work, we investigate a bilateral 4-channel transmit/receive breast coil (RAPID Biomedical GmbH, Rimpar, Germany).

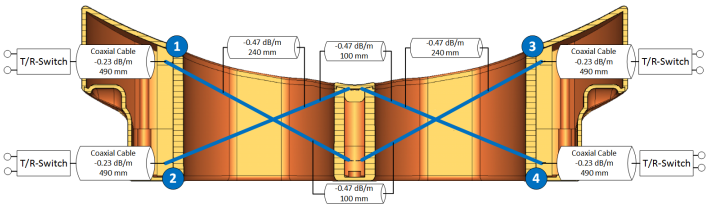

Fig. 1: Schematic of the 4-channel breast coil shown in a transversal cut through the coil housing: Layout of the four loops (blue), decoupling paths, and cable connections.

Methods: The breast coil consists of two pairs of loops in a crossed orientation with an effective angle of 44°, shown in Fig. 1 together with the coil housing ($\varepsilon_r' = 4$, $\sigma = 0.05$ S/m) as well as the internal and external coaxial cables (capacitors are not shown). The loops are tuned by capacitors placed on the loops and by a matching network at the loop's feed point. A decoupling network consisting of capacitors and coaxial cables interconnects the respective loops. The capacitors as well as the feed and decoupling networks were modelled with a network co-simulation. This enables an individual optimization of the lumped elements. For validation and fine tuning of the numerical model, which took all production tolerances into account, the simulated and measured B_1^+ maps were compared for a phantom loading the coil. The phantom, representing the upper torso and the mammae, was made from Plexiglas and was equipped with two interchangeable cups generated with a 3D printer. The phantom was filled with tissue-simulating liquid ($\varepsilon_r' = 44.84$, $\sigma = 0.76$ S/m at 297.2 MHz). Simulations were performed with CST Studio Suite 2014 (CST AG, Darmstadt, Germany). Imaging was conducted on a 7T MR system (Magnetom 7T, Siemens AG, Healthcare Sector, Erlangen, Germany) with a Bloch-Siegert shift B_1 mapping sequence [1]. The validated coil model was subsequently loaded with a heterogeneous breast model (1x1x1 mm³ voxel size) consisting of 5 tissues (bone, fat, mammary gland, muscle, skin) derived from segmented MRI images from a healthy volunteer. After optimizing the tuning, matching, and decoupling of the simulation model, B_1^+ maps for the four Tx channels were extracted. Optimized phase settings at the coil ports were determined by numerical methods with respect to improved B_1^+ uniformity inside both breasts and minimal B_1^+ variation between the left and right breast. Transmit efficiency $|B_1^+(\mathrm{ROI})|/\sqrt{P_{in}}$, max. 10g-averaged specific absorption rate $SAR_{10g,max}$, max. permissible input power $P_{in,max}$ based on the limit for the local SAR of 10 W/kg, and $|B_1^+(\mathrm{ROI})|/\sqrt{SAR_{10g,max}}$ were evaluated for the optimized phase shift settings as well as for quadrature excitation with a phase increment of 90° between the two loops of both pairs (left and right breast). The 90° phase increment results in a quadrature excitation in the center of the left and right loop pairs when loaded with an oil bottle. This was evaluated by inspection of low-tip gradient echo images without taking into account the B_1^+ variation in the oil bottle.

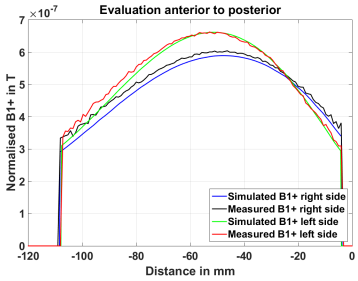

Fig. 2: Comparison of simulated and measured B_1^+ in the left and right cups on lines from anterior to posterior.

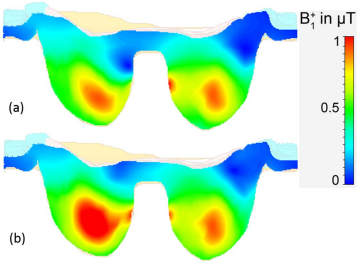

Fig. 3: B_1^+ magnitude distribution in transversal plane for (a) quadrature mode (b) optimized phase mode.

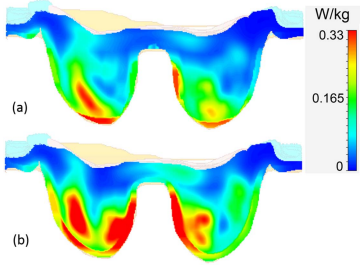

Fig. 4: 10g-averaged SAR in transversal plane for (a) quadrature mode (b) optimized phase mode.

Results: Fig. 2 exemplarily shows a comparison of the measured and simulated B_1^+ distribution in the left and right cup of the phantom on lines from anterior to posterior for $P_{in} = 1$ W and quadrature excitation with 90° phase increment. The B_1^+ distribution was evaluated on all three main axes through the center of the cups and overall a mean deviation of 3% with a (point-wise) maximum of 22% between simulation and measurement was found. This result confirms that the simulations were performed with a model of the RF coil suitable for providing realistic field distributions. Fig. 3 and 4 show a comparison of the B_1^+ distributions and the 10g-averaged SAR in the heterogeneous breast model calculated for quadrature excitation and the optimized phase setting with $P_{in} = 1$ W. Table 1 summarizes the performance parameters of the breast coil for both excitation modes in a region of interest containing the left, the right, and both breasts, respectively. Compared for both sides, the optimized mode shows 14% higher Tx efficiency with slightly better B_1^+ homogeneity, but also the max. SAR_{10g} is higher by 34%. This results in a similar $|B_1^+(\mathrm{ROI})|/\sqrt{SAR_{10g,max}}$ compared to the quadrature excitation. The left/right deviation in Tx efficiency is 2.5% and 11% for the quadrature and optimized phase mode, respectively.

Conclusion: Numerical simulations for a bilateral 4-channel transmit/receive breast coil were performed to investigate the optimum excitation mode of the coil and to determine the maximum permissible input power. Although the optimized phase mode achieves higher Tx efficiency and smaller B_1^+ variations inside the breasts, the $SAR_{10g,max}$ as well as the left/right ratio in Tx efficiency are both relatively higher. Thus, with respect to $|B_1^+(\mathrm{ROI})|/\sqrt{SAR_{10g,max}}$, both excitation modes show similar performance. However, optimization of the B_1^+ variation under constraints for the local SAR could lead to a better solution for the optimized phase mode. Further investigations will be performed with respect to B_1^+ and SAR variation for various breast anatomies as well as pathologies.

Table 1	Tx efficiency in $\mu T/\sqrt{W}$	Intra-breast variation	$SAR_{10g,max}$ in W/kg	$P_{in,max}$ in W	$\lvert B_1^+(\mathrm{ROI})\rvert/\sqrt{SAR_{10g,max}}$ in $\mu T/\sqrt{W/kg}$
Quadrature Mode	B: 0.389 / L: 0.395 / R: 0.386	B: 58% / L: 58% / R: 57%	0.59	16.6	0.506
Optimized Phase Mode	B: 0.445 / L: 0.422 / R: 0.474	B: 54% / L: 54% / R: 52%	0.794	12.3	0.499

References: 1. Sacolick et al., Magnetic Resonance in Medicine 63:1315–1322 (2010).

Acknowledgement: The research leading to these results has received funding from the European Research Council under the European Union's Seventh Framework Programme (FP/2007-2013) / ERC Grant Agreement n. 291903 MRexcite.